

Research Article

To Explore the Pathogenesis of Vascular Lesion of Type 2 Diabetes Mellitus Based on the PI3K/Akt Signaling Pathway

Jia-Rong Gao ¹, Xiu-Juan Qin,¹ Zhao-Hui Fang,² Li-Shan,¹ Li-Ping Han,¹ Hui-Jiang,¹ Ming-Fei Guo,¹ and Nan-Nan Jiang¹

¹Department of Pharmacy, The First Affiliated Hospital of Anhui University of Chinese Medicine, 117 Meishan Road, Hefei, China

²Department of Nephrology, The First Affiliated Hospital of Anhui University of Chinese Medicine, 117 Meishan Road, Hefei, China

Correspondence should be addressed to Jia-Rong Gao; zyfygir2006@163.com

Received 23 December 2018; Accepted 3 March 2019; Published 17 April 2019

Academic Editor: Bernard Portha

Copyright © 2019 Jia-Rong Gao et al. This is an open access article distributed under the Creative Commons Attribution License, which permits unrestricted use, distribution, and reproduction in any medium, provided the original work is properly cited.

Background. Type 2 diabetes mellitus (T2DM) has become a chronic disease, serious harm to human health. Complications of the blood pipe are the main cause of disability and death in diabetic patients, including vascular lesions that directly affects the prognosis of patients with diabetes and survival. This study was to determine the influence of high glucose and related mechanism of vascular lesion of type 2 diabetes mellitus pathogenesis. **Methods.** In vivo aorta abdominalis of GK rats was observed with blood pressure, heart rate, hematoxylin and eosin (H&E), Masson, and Verhoeff staining. In vitro cells were cultured with 30 mM glucose for 24 h. RT-QPCR was used to detect the mRNA expression of endothelial markers PTEN, PI3K, Akt, and VEGF. Immunofluorescence staining was used to detect the expression of PTEN, PI3K, Akt, and VEGF. PI3K and Akt phosphorylation levels were detected by Western blot analysis. **Results.** Heart rate, systolic blood pressure, diastolic blood pressure, and mean blood pressure in the GK control group were higher compared with the Wistar control group and no difference compared with the GK experimental model group. Fluorescence intensity of VEGF, Akt, and PI3K in the high-sugar stimulus group was stronger than the control group; PTEN in the high-sugar stimulus group was weakening than the control group. VEGF, Akt, and PI3K mRNA in the high-sugar stimulus group were higher than the control group; protein expressions of VEGF, Akt, and PI3K in the high-sugar stimulus group were higher than the control group. PTEN mRNA in the high-sugar stimulus group was lower than the control group. Protein expression of PTEN in the high-sugar stimulus group was lower than the control group. **Conclusions.** Angiogenesis is an important pathogenesis of T2DM vascular disease, and PTEN plays a negative regulatory role in the development of new blood vessels and can inhibit the PI3K/Akt signaling pathway.

1. Introduction

Diabetes is a common chronic disease with enhanced glucose levels occurring in the long term, which have an impact on the body and exert a number of negative effects [1]. In diabetes mellitus, glucose lipid metabolism disorders, ischemia hypoxia, inflammatory stimulation, and growth factors all promote angiogenesis. Atherosclerosis is a type of chronic pathological change in the middle arteries, which is the basis of the formation of diabetic vascular complications. Vascular endothelial dysfunction is considered to be the earliest manifestation of atherosclerosis and is a necessary initial stage of atherosclerosis [2, 3]. One previous study demonstrated that endothelial dysfunction serves a vital role in vascular disease

which is caused by diabetes mellitus [4]. The endothelium is in direct contact with the bloodstream, meaning it may become a prospective target for drug delivery.

Phosphoinositide 3-kinase (PI3K) may induce endothelial cell migration and proliferation in endothelial cells through manifold signaling pathways. PI3K-protein kinase B (Akt) signaling pathways may be a potential therapeutic method. When the oxidative stress links postprandial hyperglycaemia with endothelial dysfunction, patients with diabetes may present raised oxidant and reduced antioxidant levels [5]. The PI3K-Akt signaling pathway serves a notable role in cell apoptosis and proliferation in addition to other activities. One study confirmed that it possesses a specific role in the pathophysiology of angiopathy [6]. The activated PI3K-Akt

signaling pathway has also been demonstrated to increase insulin sensitivity, serve the role of regulating sugar lipid metabolism, and protect the vascular endothelium [7].

Endothelial cells are a key target for diabetic vascular disease. Numerous studies have demonstrated that obesity, insulin resistance, and type 2 diabetes are associated with abnormal endothelial function and participate in the occurrence and development of diabetes mellitus and small vascular complications [8]. Vascular endothelial growth factor (VEGF) is a crucial cytokine used to promote the formation of new blood vessels, which may promote vascular endothelial cells, smooth muscle cell mitosis, vascular permeability, and angiogenesis [9, 10]. Previous studies on the association between VEGF and vascular disease revealed that serum VEGF was significantly increased in patients with diabetes mellitus, and the increase of VEGF was closely associated with the germination of diabetic angiopathy [11, 12]. The present study intended to investigate the vascular lesion of type 2 diabetes mellitus in Goto-Kakizaki (GK) rats and human umbilical vein endothelial cells, in order to illustrate the mechanism of the pathogenesis of the vascular lesion of type 2 diabetes mellitus. It was hypothesized that this may provide a profound understanding of type 2 diabetes mellitus.

2. Materials and Methods

2.1. Ethics Statement. Male Wistar rats (200 ± 20 g, 5 months old, specific-pathogen-free (SPF) grade) were obtained from the Experimental Animal Center of Anhui Medical University (No. SCXK (Wan) 2011-002; Hefei, China). Spontaneous type 2 diabetes mellitus GK rats (200 ± 20 g, 5 months old, SPF grade) were obtained from the Shanghai Slix Experimental Animal Co. Ltd (No. SCXK (HU) 2012-0002). The study was approved by the ethics committee of the Experimental Animal Ethics Committee of Anhui Medical University, Hefei, China. All surgery was performed under sodium pentobarbital and minimized suffering.

2.2. Chemicals. L-Nitro-arginine-methyl-ester (L-NAME) was purchased from Sigma-Aldrich (Merck KGaA, Darmstadt, Germany; batch no. N5751-10), and sodium pentobarbital was purchased from Shanghai Chemical Reagent Co., Ltd. (Shanghai, China). Anti-HIF-1 alpha antibody, anti-PTEN antibody, anti-VEGFA antibody, anti-PI3K p85 antibody, anti-PI3K p85 (phospho Y607) antibody, and anti-AKT1 (phospho S473) antibody were purchased from Abcam (batch no. Ab1; ab32199; ab1316; ab86714; ab182651; ab81283; dilution 1:200; 1:100; 1:100; 1:100; 1:200; 1:200); TRIB3 polyclonal antibody, AKT (L321) polyclonal antibody, and AKT (phospho-T308) polyclonal antibody were purchased from Bioworld (batch no. BS60451; BS1502; BS4647; dilution 1:100; 1:100; 1:100).

2.3. Animal Experiments and Sample Collection. All rats were allowed *ad libitum* access to food and water and a separate room in a facility at a temperature of 18–22°C and humidity of 40–60%. The Wistar rats were administered regular feed, and the GK rats were fed a high-fat feed (as follows: normal

feed, 88.2%; refined lard, 10%; cholesterol, 1.5%; and pig bile salt, 0.3%). Subsequent to acclimatization for 1 week, the caudal edge of the liver in GK rats exhibited a high blood flow when the rats were awake and the blood glucose of the GK rats was determined using a Roche glucose meter (Roche Diagnostics, Basel, Switzerland). The standard of type 2 diabetes mellitus is blood sugar > 11.1 mmol/l, and the results met these criteria. The rats were randomly divided into a GK control group ($n = 10$), a GK experimental model group ($n = 10$), and a Wistar control group ($n = 10$). The drinking water from the GK experimental model group had L-NAME (0.1 mg/kg) added to it for continuous molding for 42 days. All rats were anesthetized with sodium pentobarbital (30 mg/kg, intraperitoneal injection), and abdominal aortic tissues were sealed and stored at -80°C. All rats were euthanized prior to this isolation of aortic tissue by cervical dislocation.

2.4. Cell Culture. Human umbilical vein endothelial cells were cultured in RPMI-1640 medium (Thermo Fisher Scientific, Inc., Waltham, MA, USA) with 10% fetal bovine serum and 1% penicillin/streptomycin (Sigma-Aldrich; Merck KGaA). Cells were incubated under 5% CO₂ at 37°C; normal medium was 5.5% glucose.

2.5. MTT Cell Experiment. The cell seed plate was treated with drug addiction according to the experimental scheme, and the concentration of each sample was set to 3–5 replications. 20 milliliters of 1 MTT solution (5 mg/ml, i.e., 0.5% MTT) was added to all holes and incubated in the incubator for 4 hours. Carefully remove the supernatant and add DMSO (dimethylsulphoxide) at 150 milligrams per well for 10 min at low speed (120~140 rpm/min) in the shaking table for full dissolution of the crystals. The absorptive value of 490 nm was measured using an enzyme labelling machine, and the inhibition rate of the drug on cells was calculated according to the formula.

2.6. Blood Pressure and Heart Rate Analysis. Systolic blood pressure, diastolic blood pressure, mean blood pressure, and heart rate of the rats were monitored using a tail blood pressure measuring instrument, and the mean blood pressure of each animal was measured three times.

2.7. Histological Analysis. A right lobe of each aorta abdominalis tissue from each rat was fixed in 10% neutral formalin and stained with hematoxylin and eosin (H&E), Masson, and Verhoeff staining for histological examination.

2.8. Immunofluorescence Analysis. Initially, subsequent to drying, the cells were evenly distributed in the center of the cover glass with a group pen; 50–100 μl of the membrane working fluid was added to each dish, incubated at room temperature for 20 min, and then washed with phosphate buffered saline (PBS) for 5 min each time. The tissue was then evenly covered with 3% bovine serum albumin in the ring, and the temperature was maintained for 30 min at room temperature. Following this, the cells were gently shaken with the sealing fluid in the orifice plate, mixed with PBS, and then the cell culture plate was placed flat on a wet box at 4°C for

TABLE 1: Real-time quantitative PCR primer sequence.

Gene name	GeneBank ID	Sense primer	Antisense primer	Product length
Akt	NM_005163	GCACAAACGAGGGGAGTACAT	AGCGGATGATGAAGGTGTTGG	192
PI3K	NM_181523	ACCACTACCGGAATGAATCTCT	GGGATGTGCGGGTATATTCTTC	207
PENT	NM_000314	AGGGACGAACTGGTGTAAATGA	CTGGTCCTTACTTCCCCATAGAA	100
VEGF	NM_001171627	AGGGCAGAATCATCACGAAGT	AGGGTCTCGATTGGATGGCA	75
ACTA	NM_001101	CATGTACGTTGCTATCCAGGC	CTCCTTAATGTACGCACGAT	250

TABLE 2: MTT cell experiment data.

Group	OD average (24 h)	OD average (48 h)	Inhibition ratio (24 h)	Inhibition ratio (48 h)
Normal HUVEC	0.87	1.17	—	—
30 mM high glucose group	0.84	0.94	0.03	0.19
5.5 mM glucose + 24.5 mM mannitol high osmotic pressure group	0.84	0.94	0.03	0.20
5% drug serum	0.85	1.06	0.03	0.09
10% drug serum	0.81	0.92	0.07	0.21
15% drug serum	0.78	0.81	0.11	0.31
20% drug serum	0.68	0.73	0.22	0.38
25% drug serum	0.62	0.54	0.29	0.54
30% drug serum	0.53	0.50	0.39	0.57

TABLE 3: The SBP, DBP, MBP, and HR of rats ($n = 10$).

	Wistar control group	GK control group	GK experimental model group
SBP	128.37 ± 4.92	185.20 ± 10.06**	187.31 ± 10.29
DBP	117.86 ± 5.45	167.45 ± 6.73**	162.72 ± 7.93
MBP	124.86 ± 4.14	179.28 ± 6.12**	179.11 ± 6.71
HR	327.10 ± 12.16	442.20 ± 17.77**	439.00 ± 24.32

Note: compared with the control group, ** $P < 0.05$.

incubation overnight. The cell orifice plate was then placed on the decolorized rocking bed 3 times for 5 min each time. Following drying, the two antioated tissues of the corresponding species in the inner circle were incubated for 50 min. The slide was then placed in PBS (pH 7.4) and washed three times on the decolorized bed for 5 min each time. Once the section was dried, DAPI dye was added to the ring and incubated for 10 min. The slide was then placed in PBS (pH 7.4) and washed three times on the decolorized bed for 5 min each time. The glass slide was dried and then sealed with antifluorescence quenching. The images were observed and collected under a fluorescence microscope.

2.9. Reverse Transcriptase-Quantitative Polymerase Chain Reaction (RT-qPCR) Analysis. TRIzol reagent (Invitrogen; Thermo Fisher Scientific, Inc.) was used to isolate and purify total RNA according to the manufacturer's protocol. The quantity and quality of the RNA samples were determined using the NanoDrop 2000 instrument (Thermo Fisher Scientific, Inc.). The RNA integrity was assessed by electrophoresis with denaturing agarose gel.

RT-qPCR was performed using a fluorescence quantitative PCR instrument (ABI 7300) according to the manufacturer's

protocol. β -Actin was used as a control. All PCR primers used are listed in Table 1. All experiments were performed in triplicate. The data was analyzed using the $2^{-\Delta\Delta C_q}$ method.

2.10. Western Blot Analysis. Cells were scraped and lysed in RIPA buffer (cat no. P0013B; Beyotime Institute of Biotechnology, Haimen, China), and proteins were measured with a bicinchoninic acid protein assay kit (cat no. P0010; Beyotime Institute of Biotechnology). The primary antibodies used in the experiments are as follows: Akt (cat no. BS2987, 1:500; Bioworld Technology, Inc., St. Louis Park, MN, USA), VEGF (cat no. ab1316, 1:150; Abcam, Cambridge, UK), phosphatase and tensin homolog (PTEN; cat no. ab32199, 1:500; Abcam), and β -actin (cat no. ab8226, 1:2,000; Abcam), followed by horseradish peroxidase-conjugated secondary antibodies (cat no. A0208, 1:1,000; Beyotime Institute of Biotechnology). Protein bands were visualized using electrochemiluminescence reagents (cat no. P0018; Beyotime Institute of Technology).

2.11. Statistical Analysis. Experimental data were presented as the mean ± standard deviation. Statistical comparisons were performed using Student's t -test, and $P < 0.05$ was considered to indicate a statistically significant difference.

3. Results

3.1. MTT Cell Experiment Result. MTT data showed that high glucose has inhibited cell activity (Table 2).

3.2. Blood Pressure and Heart Rate. The heart rate results in the rats revealed that the heart rate of the GK control group was significantly higher compared with in the Wistar control group ($P < 0.05$), but no significant difference was identified when compared with the GK experimental model group.

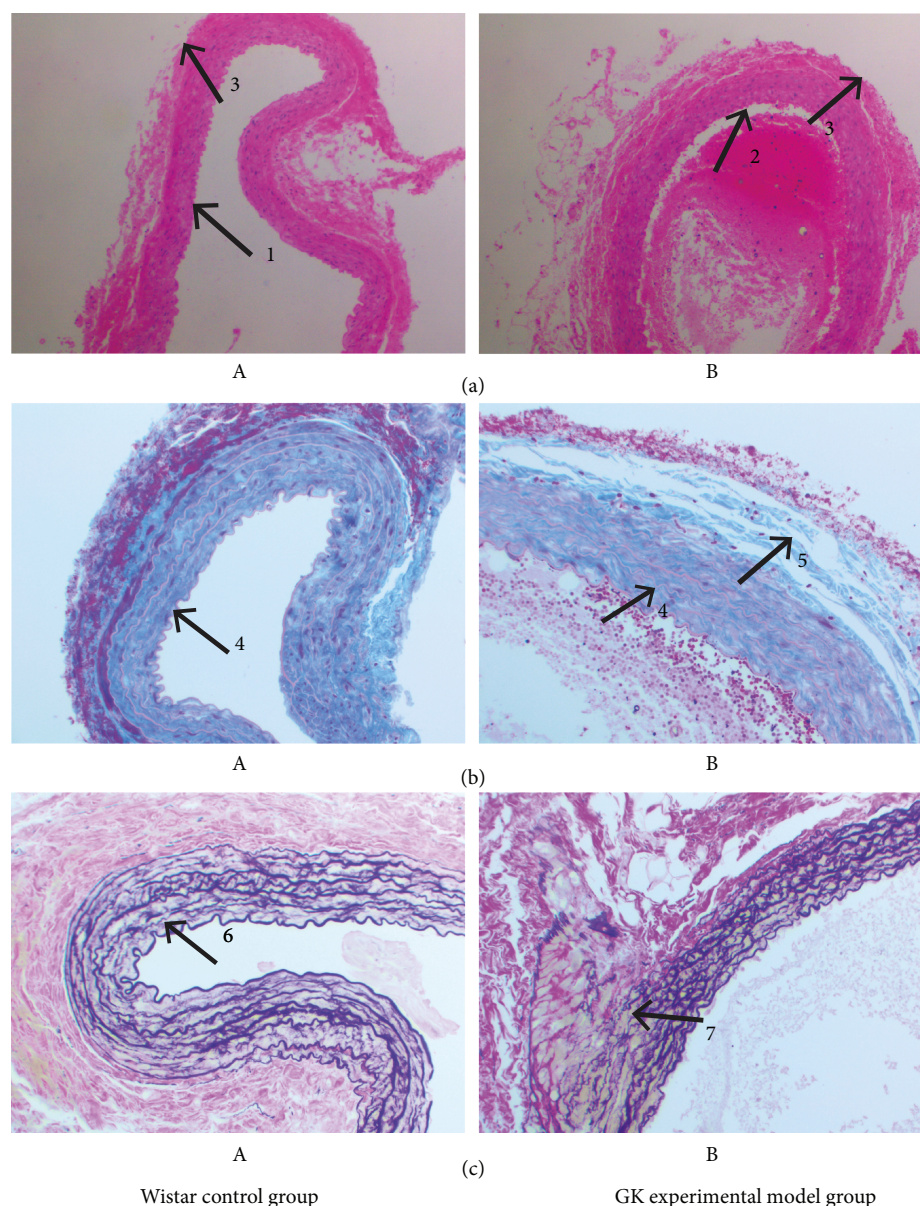


FIGURE 1: Histological examination of the aorta abdominalis tissue of type 2 diabetes mellitus in rats (magnification $\times 200$). (a) H&E staining; (b) Masson staining; (c) Verhoeff staining; A: Wistar control group; B: GK experimental model group. 1: endothelium cells; 2: swollen and infiltrated endothelium cells; 3: media thickness; 4: collagen fibers; 5: peritubular collagen fibers; 6: elastic fibers; 7: elastic fiber fracture.

Similarly, systolic blood pressure in the GK control group was significantly higher compared with the Wistar control group ($P < 0.05$), but no significant difference was identified compared with the GK experimental model group.

Additionally, diastolic blood pressure in the GK control group was significantly higher when compared with that of the Wistar control group ($P < 0.05$), but not compared with the GK experimental model group. Finally, the mean blood pressure in the GK control group was significantly higher when compared with that of the Wistar control group ($P < 0.05$), but not when compared with the GK experimental model group (Table 3).

3.3. Histopathology. H&E staining revealed that the rats in the Wistar control group presented with a flat abdominal aorta

intima and flat endothelial cells, clingy on flat in elastic plate, neatly and elastic plate with smooth muscle cells in parallel arrangement, intimal smooth and tidy. Compared with the control group, there was thickening and breakage of the intima, the endothelial cells were partially detached, swollen, and infiltrated in the rats in the GK experimental model group. Additionally, the smooth muscle cells of the medium membrane had undergone hypertrophy, were distorted, and had an arranged disorder, and the number of layers was increased (Figure 1(a)).

Masson staining revealed that the aortic smooth muscle cells and elastic fibers were dyed red and the collagen fibers were blue-green. Rats from the Wistar control group demonstrated that the collagenous fibers of the abdominal aorta wall are evenly distributed and are slender and the adjacent cells have a good network of collagen fibers. The fibrosis of the

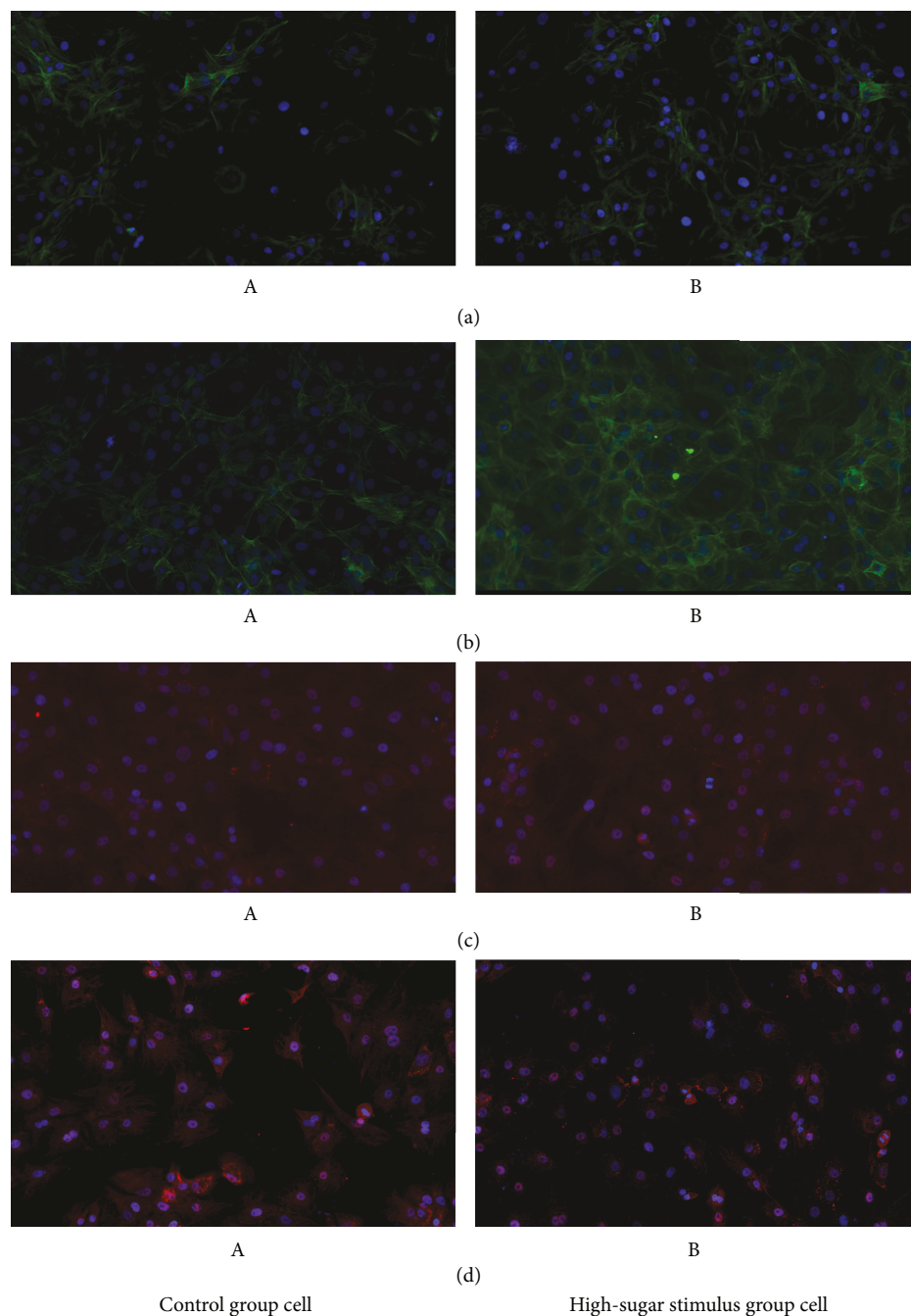


FIGURE 2: Immunofluorescence analysis of HUVEC cells (magnification $\times 200$). (a) VEGF; (b) AKT; (c) PI3K; (d) PTEN; A: control group cell; B: high-sugar stimulus group.

vessels was very light. Compared with the control group, the collagenous fibers of the abdominal aorta were increased, and the collagen fibers were interlinked into nets or clumps and arranged in a disordered and unevenly distributed manner, tightly surrounding the smooth muscle cells in the rats of the GK experimental model group (Figure 1(b)).

Verhoeff staining revealed that the membrane elastic fibers in the aorta were black or blue-black and the smooth muscle fibers and collagen fibers were red. Rats from the Wistar control group revealed that the abdominal aorta elastic fiber distribution was uniform, neat, and complete without fracture.

Compared with the control group, the abdominal aorta elastic fibers were circular, the arrangement was loose, the distribution was unevenly distributed, and the visible fracture was notable in the rats of the GK experimental model group (Figure 1(c)).

3.4. Fluorescence Intensity Results. Under a confocal microscope, the expression of VEGF, PTEN, PI3K, and Akt in the cells produced blue fluorescence; VEGF in the control group cells produced comparatively weak fluorescence and an enhanced fluorescence intensity in the high-sugar stimulus group. The PI3K and Akt expression in the control group

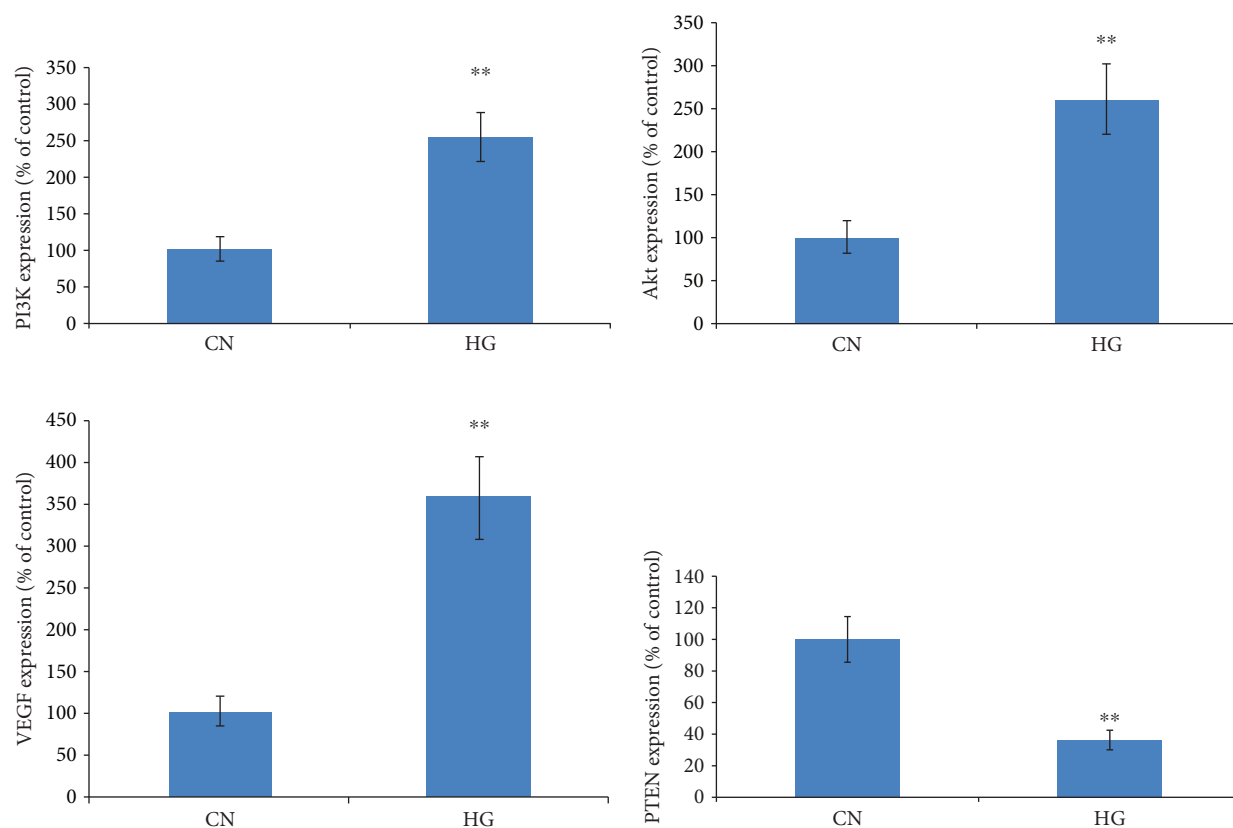


FIGURE 3: The relative expression of VEGF, AKT, PI3K, and PTEN in immunofluorescence analysis. Compared with the control group, ** $P < 0.01$.

cell demonstrated weak fluorescence and enhanced fluorescence intensity in the high-sugar stimulus group. PTEN in the control group cell demonstrated strong fluorescence, and the fluorescence intensity of the high-sugar stimulus group was comparatively weak (Figures 2 and 3).

3.5. mRNA Expression Level Results. The amplification curve revealed that in the present study, the reaction curves of PTEN, Akt, PI3K, and VEGF were substantial, and these exhibited high efficiency rates and good parallelism of amplification curve. Additionally, a repeated reaction produced a similar level of amplification, demonstrating the efficiency, repeatability, and accuracy of this experiment. The low concentration curve index period is obvious, not easy to appear false masculine misjudgment, and had high sensitivity. The melting curve revealed a curve with a single peak, indicating that the amplification product was pure. The product length met the design requirements, indicating that the C_q value produced was accurate.

RT-qPCR revealed that PTEN mRNA expression levels in the high-sugar stimulus group were significantly lower compared with the control group ($P < 0.01$) and that the mRNA expression levels of PI3K, Akt, and VEGF in the high-sugar stimulus group were significantly higher compared with the control group ($P < 0.01$) (Figure 4).

3.6. Protein Expression Level Results. Western blot analysis revealed that the protein expression levels of PTEN in the high-sugar stimulus group were significantly lower compared

with the control group ($P < 0.01$) and the protein expression levels of PI3K, Akt, and VEGF in the high-sugar stimulus group were significantly higher compared with the control group ($P < 0.01$) (Figure 5).

4. Discussion

GK rats are internationally recognized nonobesity type 2 diabetes mellitus animal models with the following characteristics: lower glucose-stimulated insulin secretion, excessive liver sugar production, and muscle and adipose tissue medium insulin resistance [13, 14]. The administration of the nitric oxide (NO) synthase inhibitor L-NAME for extended periods of time may inhibit endothelial NO synthesis, damage vascular endothelial function, and induce the expression of cytokines including VEGF in order to study animal models of type 2 diabetes mellitus and their large vascular lesions [15, 16]. L-NAME could further induce the vascular disease, which was administered in an animal study. In the present study, the heart rate, systolic blood pressure, diastolic blood pressure, and mean blood pressure were assessed and were revealed to be higher in the GK control group compared with the Wistar control group; and no difference was revealed when compared with the GK experimental model group. H&E, Masson's, and Verhoeff staining revealed that the rats from the GK experimental model group had damage at different levels.

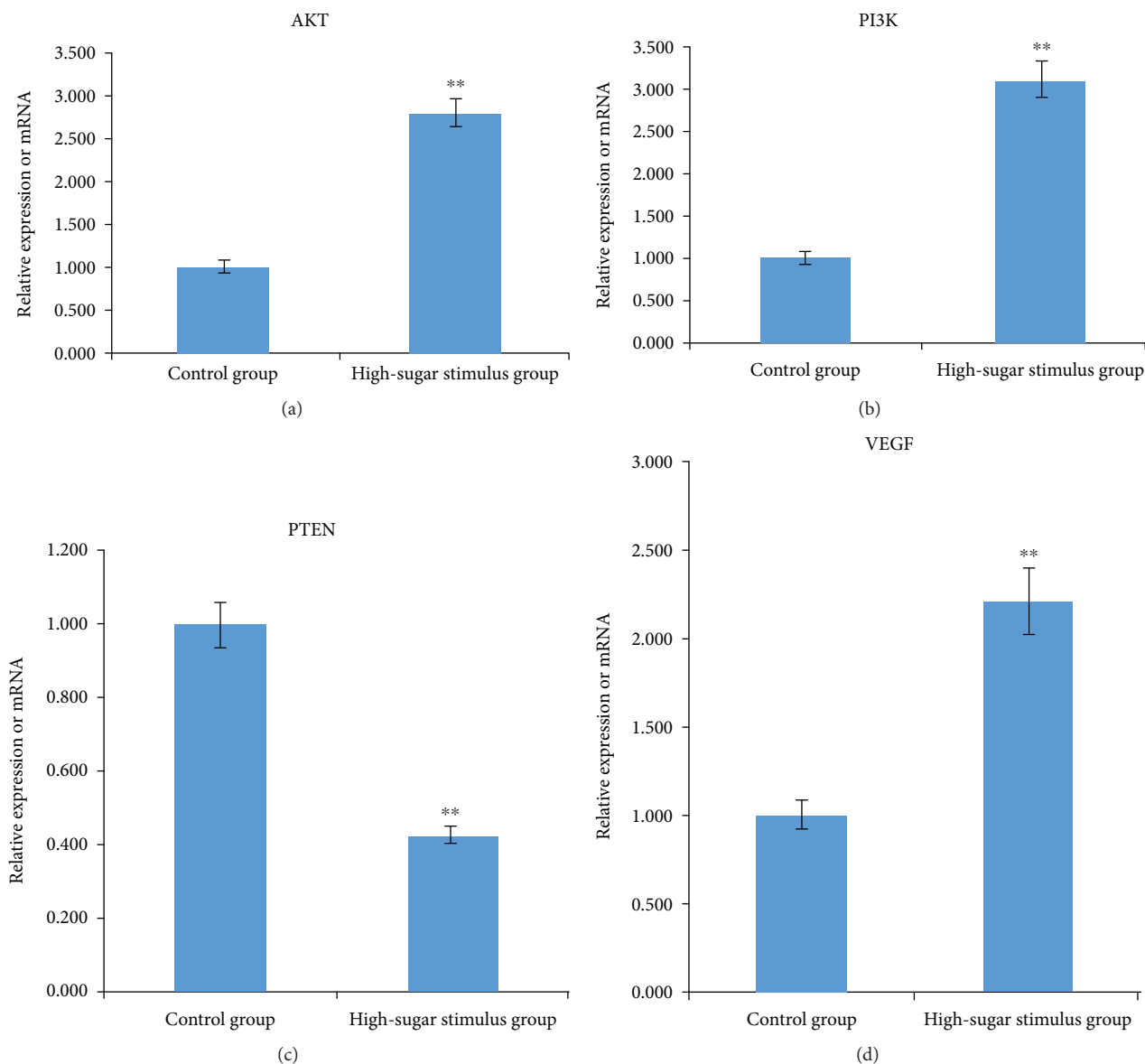


FIGURE 4: The expression of VEGF, AKT, PI3K, and PTEN mRNA in HUVEC cells. Compared with the control group, ** $P < 0.01$.

Vascular endothelial cells are highly differentiated monolayer cells which cover the surface of the vascular lumen and serve important functions including regulating vascular permeability, maintaining blood flow, and regulating vascular smooth muscle cell proliferation. Endothelial cell apoptosis may increase smooth muscle cell proliferation and migration, enhance blood coagulation, and increase leukocyte infiltration into the endothelium thus leading to endothelial dysfunction [17, 18]. Multiple metabolic disorders in type 2 diabetes mellitus accelerate this pathophysiological process. In the state of diabetes, numerous factors including high blood sugar levels, glycation end products being produced, ischemia, and hypoxia promote the expression of cytokines associated with angiogenesis [19]. The dysfunction of endothelial cells has become an important initial factor for the development of type 2 diabetes mellitus and its vascular complications. Additionally, atherosclerosis is a type of chronic

pathological change in the middle arteries, which is the basis of the formation of a diabetic vascular system [20, 21].

VEGF is a glycosylated mitogen that specifically affects endothelial cells and has various effects, including mediating increased vascular permeability, inducing angiogenesis, vasculogenesis, and endothelial cell growth, promoting cell migration, and inhibiting apoptosis [22–24]. VEGF additionally mediates vascular endothelial permeability and proliferation [25]. In the present study, the fluorescence intensity, protein expression, and mRNA expression of VEGF in the high-sugar stimulus group were higher compared with the control group. These results illustrate that angiogenesis is an important aspect of the pathogenesis of type 2 diabetes mellitus vascular disease.

PTEN is a tumor suppressor which is mutated in a number of different cancer types at a high frequency. Phosphatidylinositol-3,4,5-trisphosphate 3-phosphatase is encoded by this gene. This protein dephosphorylates

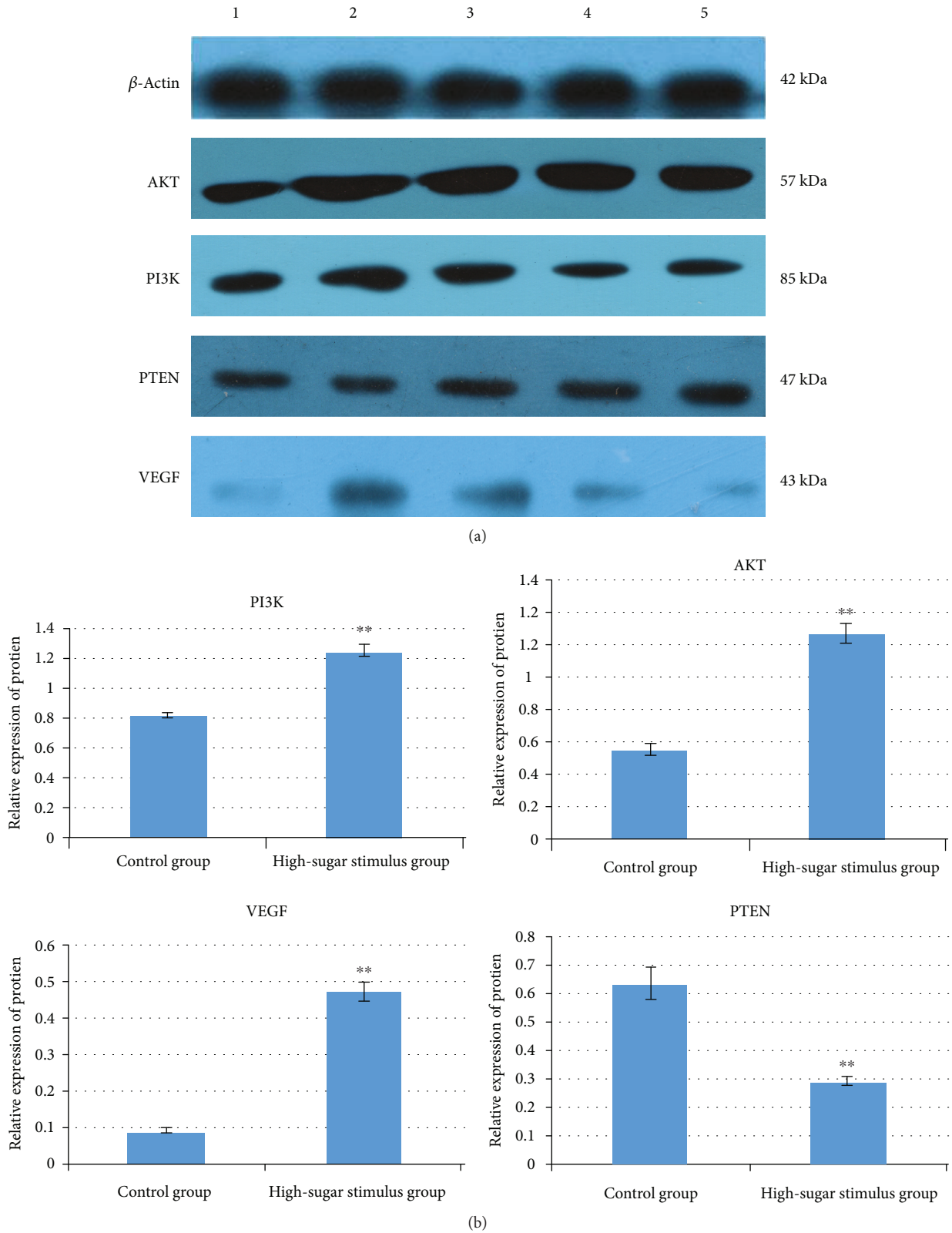


FIGURE 5: Western blot analysis of VEGF, AKT, PI3K, and PTEN protein (a). The expression of VEGF, AKT, PI3K, and PTEN protein in HUVEC cells (b). Compared with the control group, ** $P < 0.01$.

phosphoinositide substrates unlike other protein tyrosine phosphatases [26]. It functions as a tumor suppressor and regulates intracellular levels of phosphatidylinositol-3,4,5-

trisphosphate in cells by negatively regulating the Akt signaling pathway. This also regulates energy metabolism in the mitochondria [27, 28].

Angiogenesis is a tyrosine kinase and its ligand signals through a complicated endothelial molecular system, and this ligand signaling system regulates the endothelial cell function, including endothelial cell proliferation, migration, and capillary formation [29]. The VEGF/VEGF receptor signaling system controls these processes and is closely associated with the PI3K signaling pathway [30, 31]. PI3K is activated on the membrane subsequent to the generation of phosphatidylinositol triphosphate (PIP3), resulting in the activation of downstream proteins including Akt which serve a vital role in the process of angiogenesis. PIP3 is the target molecule of phosphatase action, which is the key component of the cell growth regulation pathway. The main function is to stimulate cell growth and block apoptosis [32, 33]. PTEN produces PIP3 for phosphorylation and inhibits the phosphorylation of the PI3K kinase, thereby blocking the Akt signaling pathway, blocking the downstream enzyme activity, and regulating the endothelial cells' VEGF signaling pathways and cellular response. Therefore, PTEN serves a negative regulatory role in the development of novel blood vessels [34]. By inhibiting the PI3K/Akt signaling pathway, PTEN serves an inhibitory role in the formation and development of the pathological neovascularization of atherosclerotic plaques [35–37].

In the present study, the fluorescence intensity of Akt and PI3K in the high-sugar stimulus group was stronger compared with the control group, and that of PTEN in the high-sugar stimulus group was weaker compared with the control group. Akt and PI3K mRNA and protein expression in the high-sugar stimulus group were higher compared with the control group, and that of PTEN mRNA in the high-sugar stimulus group was lower compared with the control group. These results illustrate that PTEN serves a negative regulatory role in the development of novel blood vessels and may inhibit the PI3K/Akt signaling pathway. It inhibits the formation and development of the pathological neovascularization of an atheromatous plaque.

In summary, when vascular disease occurred in type 2 diabetes rats, the expression of VEGF in the aortic tissue was increased, the expression of PTEN was decreased, and the activity of the PI3K/Akt signaling pathway was decreased. Excessive proliferation of vascular endothelial cells is a common model in diabetic vascular disease. Therefore, inhibiting excessive proliferation of vascular endothelial cells is conducive to the effective control of diabetic vascular disease. This study furthered the understanding of the mechanisms of type 2 diabetes and produced a potential method for future disease treatment studies, which may contribute to the development of novel diagnostic markers and therapeutic targets for the clinic treatment of type 2 diabetes. However, there were still some limitations in the current study. Glucose metabolism is mainly detected when insulin resistance mechanism is performed, while we focus on vascular lesions, so nevertheless, further experiments are required to validate their effects in type 2 diabetes. At the present stage, we mainly want to explain the mechanism of damage to large vessels, especially endothelial cells in the process of diabetes. We are also designing and carrying out the mechanism of the regulation of angiogenesis by antihypertensive drugs.

Data Availability

The data used to support the findings of this study are available from the corresponding author upon request.

Conflicts of Interest

The authors declare that they have no conflicts of interest.

Authors' Contributions

JR G conceived and designed the study. NN J, LP H, and MF G performed the experiments. XJ Q wrote the paper. H J, ZH F, and L S reviewed and edited the manuscript. All authors read and approved the manuscript.

Acknowledgments

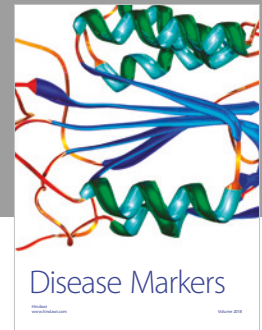
This study was financially supported by Science Foundation Projects of Anhui University of Traditional Chinese Medicine (2014qn018) and the second batch of scientific research projects of the national TCM clinical research base of the State Administration of Traditional Chinese Medicine (JDZX2015126). We are grateful to Mr. Qiang Fan (Ao Ji Bio-tech Co., Ltd., Shanghai, China) for providing help in data analysis.

References

- [1] Z. Du, Z. Qiu, Z. Wang, and X. Wang, "The inhibitory effects of soybean isoflavones on testicular cell apoptosis in mice with type 2 diabetes," *Experimental and Therapeutic Medicine*, vol. 15, no. 1, pp. 305–309, 2018.
- [2] M. van den Heuvel, O. Sorop, N. S. van Ditzhuijzen et al., "The effect of bioresorbable vascular scaffold implantation on distal coronary endothelial function in dyslipidemic swine with and without diabetes," *International Journal of Cardiology*, vol. 252, pp. 44–51, 2018.
- [3] M. Jamilian, M. Samimi, F. Afshar Ebrahimi et al., "Effects of selenium supplementation on gene expression levels of inflammatory cytokines and vascular endothelial growth factor in patients with gestational diabetes," *Biological Trace Element Research*, vol. 181, no. 2, pp. 199–206, 2018.
- [4] V. Sudhakar, M. N. Okur, Z. Bagi et al., "Akt2 (protein kinase B beta) stabilizes ATP7A, a copper transporter for extracellular superoxide dismutase, in vascular smooth muscle: novel mechanism to limit endothelial dysfunction in type 2 diabetes mellitus," *Arteriosclerosis, Thrombosis, and Vascular Biology*, vol. 38, no. 3, pp. 529–541, 2018.
- [5] J. Cui, R. Gong, S. Hu, L. Cai, and L. Chen, "Gambogic acid ameliorates diabetes-induced proliferative retinopathy through inhibition of the HIF-1 α /VEGF expression via targeting PI3K/AKT pathway," *Life Sciences*, vol. 192, pp. 293–303, 2018.
- [6] J. Choi, K. J. Kim, E. J. Koh, and B. Y. Lee, "Gelidium elegans extract ameliorates type 2 diabetes via regulation of MAPK and PI3K/Akt signaling," *Nutrients*, vol. 10, no. 1, 2018.
- [7] C. Feng, Z. Jin, X. Chi et al., "SHBG expression is correlated with PI3K/AKT pathway activity in a cellular model of human insulin resistance," *Gynecological Endocrinology*, vol. 34, no. 7, pp. 567–573, 2018.

- [8] M. E. Francois, E. Myette-Cote, T. D. Bammert et al., "Carbohydrate restriction with postmeal walking effectively mitigates postprandial hyperglycemia and improves endothelial function in type 2 diabetes," *American Journal of Physiology-Heart and Circulatory Physiology*, vol. 314, no. 1, pp. H105–H113, 2018.
- [9] H.-Y. Cai, L. Li, T. Guo et al., "Cardiac shockwave therapy improves myocardial function in patients with refractory coronary artery disease by promoting VEGF and IL-8 secretion to mediate the proliferation of endothelial progenitor cells," *Experimental and Therapeutic Medicine*, vol. 10, no. 6, pp. 2410–2416, 2015.
- [10] Q. Li, S. Xia, H. Fang, J. Pan, Y. Jia, and G. Deng, "VEGF treatment promotes bone marrow-derived CXCR4⁺ mesenchymal stromal stem cell differentiation into vessel endothelial cells," *Experimental and Therapeutic Medicine*, vol. 13, no. 2, pp. 449–454, 2017.
- [11] R. Terzić, I. Cilenšek, R. Z. Pleskovič, S. Mankoč, and A. Milutinović, "Vascular endothelial growth factor (VEGF)-related single nucleotide polymorphisms rs10738760 and rs6921438 are not associated with diabetic retinopathy (DR) in Slovenian patients with type 2 diabetes mellitus (T2DM)," *Bosnian Journal of Basic Medical Sciences*, vol. 17, no. 4, pp. 328–332, 2017.
- [12] B. Zhang, D. Wang, T. F. Ji, L. Shi, and J. L. Yu, "Overexpression of lncRNA ANRIL up-regulates VEGF expression and promotes angiogenesis of diabetes mellitus combined with cerebral infarction by activating NF- κ B signaling pathway in a rat model," *Oncotarget*, vol. 8, no. 10, pp. 17347–17359, 2017.
- [13] Y. Toyoda, Y. Ito, K. Tanigawa, and I. Miwa, "Impairment of glucokinase translocation in cultured hepatocytes from OLETF and GK rats, animal models of type 2 diabetes," *Archives of Histology and Cytology*, vol. 63, no. 3, pp. 243–248, 2000.
- [14] Y. Liu, C. G. Xie, and M. Chen, "Effect of Shenqi compound on PTEN/PI3K signal transduction in GK rats with diabetes mellitus macroangiopathy," *Zhongguo Zhong Xi Yi Jie He Za Zhi*, vol. 30, no. 6, pp. 640–644, 2010.
- [15] N. Tekin, F. Akyuz, and H. E. Temel, "NO levels in diabetes mellitus: effects of l-NAME and insulin on LCAT, Na⁺/K⁺ ATPase activity and lipid profile," *Diabetes & Metabolic Syndrome: Clinical Research & Reviews*, vol. 5, no. 4, pp. 191–195, 2011.
- [16] M. Haluzik, J. Nedvidkova, and J. Skrha, "The influence of methylene blue and L-NAME on the development of streptozotocin-induced diabetes in rats," *Sbornik Lekarsky*, vol. 100, no. 3, pp. 213–217, 1999.
- [17] H. M. Zhou, Q. X. Sun, and Y. Cheng, "Paeonol enhances the sensitivity of human ovarian cancer cells to radiotherapy-induced apoptosis due to downregulation of the phosphatidylinositol-3-kinase/Akt/phosphatase and tensin homolog pathway and inhibition of vascular endothelial growth factor," *Experimental and Therapeutic Medicine*, vol. 14, no. 4, pp. 3213–3220, 2017.
- [18] L. Yang and C. Gao, "MiR-590 Inhibits Endothelial Cell Apoptosis by Inactivating the TLR4/NF- κ B Pathway in Atherosclerosis," *Yonsei Medical Journal*, vol. 60, no. 3, pp. 298–307, 2019.
- [19] S. Margaryan, A. Witkowicz, A. Partyka, L. Yepiskoposyan, G. Manukyan, and L. Karabon, "The mRNA expression levels of uncoupling proteins 1 and 2 in mononuclear cells from patients with metabolic disorders: obesity and type 2 diabetes mellitus," *Postępy Higieny i Medycyny Doświadczalnej*, vol. 71, pp. 895–900, 2017.
- [20] K. E. Bornfeldt, F. Kramer, A. Batorsky et al., "A novel type 2 diabetes mouse model of combined diabetic kidney disease and atherosclerosis," *The American Journal of Pathology*, vol. 188, no. 2, pp. 343–352, 2018.
- [21] N. Katakami, "Mechanism of development of atherosclerosis and cardiovascular disease in diabetes mellitus," *Journal of Atherosclerosis and Thrombosis*, vol. 25, no. 1, pp. 27–39, 2018.
- [22] Z. Cheng, J. Fu, G. Liu, L. Zhang, Q. Xu, and S. Y. Wang, "Angiogenesis in JAK2 V617F positive myeloproliferative neoplasms and ruxolitinib decrease VEGF, HIF-1 expression in JAK2 V617F positive cells," *Leukemia & Lymphoma*, vol. 59, no. 1, pp. 196–203, 2018.
- [23] S. Lakshmikanthan, M. Sobczak, S. Li Calzi, L. Shaw, M. B. Grant, and M. Chrzanowska-Wodnicka, "Rap1B promotes VEGF-induced endothelial permeability and is required for dynamic regulation of the endothelial barrier," *Journal of Cell Science*, vol. 131, no. 1, article jcs207605, 2018.
- [24] A. K. Pandey, E. K. Singhi, J. P. Arroyo et al., "Mechanisms of VEGF (vascular endothelial growth factor) inhibitor-associated hypertension and vascular disease," *Hypertension*, vol. 71, no. 2, pp. e1–e8, 2018.
- [25] Z. Li, Y. Zhang, Y. Liao, R. Zeng, P. Zeng, and Y. Lan, "Comparison of efficacy between anti-vascular endothelial growth factor (VEGF) and laser treatment in type-1 and threshold retinopathy of prematurity (ROP)," *BMC Ophthalmology*, vol. 18, no. 1, p. 19, 2018.
- [26] E. Kashiwagi, S. Inoue, T. Mizushima et al., "Prostaglandin receptors induce urothelial tumorigenesis as well as bladder cancer progression and cisplatin resistance presumably via modulating PTEN expression," *British Journal of Cancer*, vol. 118, no. 2, pp. 213–223, 2017.
- [27] P. A. Perez, J. P. Petiti, F. Picech et al., "Estrogen receptor β regulates the tumoral suppressor PTEN to modulate pituitary cell growth," *Journal of Cellular Physiology*, vol. 233, no. 2, pp. 1402–1413, 2018.
- [28] J. Ramirez-Moya, L. Wert-Lamas, and P. Santisteban, "MicroRNA-146b promotes PI3K/AKT pathway hyperactivation and thyroid cancer progression by targeting PTEN," *Oncogene*, vol. 37, no. 25, pp. 3369–3383, 2018.
- [29] H. P. Lee, Y. C. Liu, P. C. Chen et al., "Tanshinone IIA inhibits angiogenesis in human endothelial progenitor cells *in vitro* and *in vivo*," *Oncotarget*, vol. 8, no. 65, pp. 109217–109227, 2017.
- [30] Y. Huang, Y. Mao, H. Li, G. Shen, and G. Nan, "Knockdown of Nrf2 inhibits angiogenesis by down-regulating VEGF expression through PI3K/Akt signaling pathway in cerebral microvascular endothelial cells under hypoxic conditions," *Biochemistry and Cell Biology*, vol. 96, no. 4, pp. 475–482, 2018.
- [31] X. Ma, H. Yao, Y. Yang et al., "miR-195 suppresses abdominal aortic aneurysm through the TNF- α /NF- κ B and VEGF/PI3K/Akt pathway," *International Journal of Molecular Medicine*, vol. 41, no. 4, pp. 2350–2358, 2018.
- [32] B. Cai, Y. Zheng, S. Ma et al., "Long non-coding RNA regulates hair follicle stem cell proliferation and differentiation through PI3K/AKT signal pathway," *Molecular Medicine Reports*, vol. 17, no. 4, pp. 5477–5483, 2018.
- [33] J. Li, B. Xu, Z. Chen et al., "PI3K/AKT/JNK/p38 signalling pathway-mediated neural apoptosis in the prefrontal cortex

- of mice is involved in the antidepressant-like effect of pioglitazone,” *Clinical and Experimental Pharmacology and Physiology*, vol. 45, no. 6, pp. 525–535, 2018.
- [34] H. Pan, T. Li, Y. Jiang et al., “Overexpression of circular RNA ciRS-7 abrogates the tumor suppressive effect of miR-7 on gastric cancer via PTEN/PI3K/AKT signaling pathway,” *Journal of Cellular Biochemistry*, vol. 119, no. 1, pp. 440–446, 2018.
- [35] B. H. Jiang and L. Z. Liu, “Chapter 2 PI3K/PTEN signaling in angiogenesis and tumorigenesis,” *Advances in Cancer Research*, vol. 102, pp. 19–65, 2009.
- [36] K. Hamada, T. Sasaki, P. A. Koni et al., “The PTEN/PI3K pathway governs normal vascular development and tumor angiogenesis,” *Genes & Development*, vol. 19, no. 17, pp. 2054–2065, 2005.
- [37] J. Shang and Z. Zhao, “Emerging role of HuR in inflammatory response in kidney diseases,” *Acta Biochimica et Biophysica Sinica*, vol. 49, no. 9, pp. 753–763, 2017.



Hindawi

Submit your manuscripts at
www.hindawi.com

